Multifrequency Sp Stacking Reveals a Strong Asthenospheric Discontinuity beneath the Anatolian Region

J. Hua[1] (junlin_hua@brown.edu), K. M. Fischer[1], M. Wu[1] and N. Blom[2]

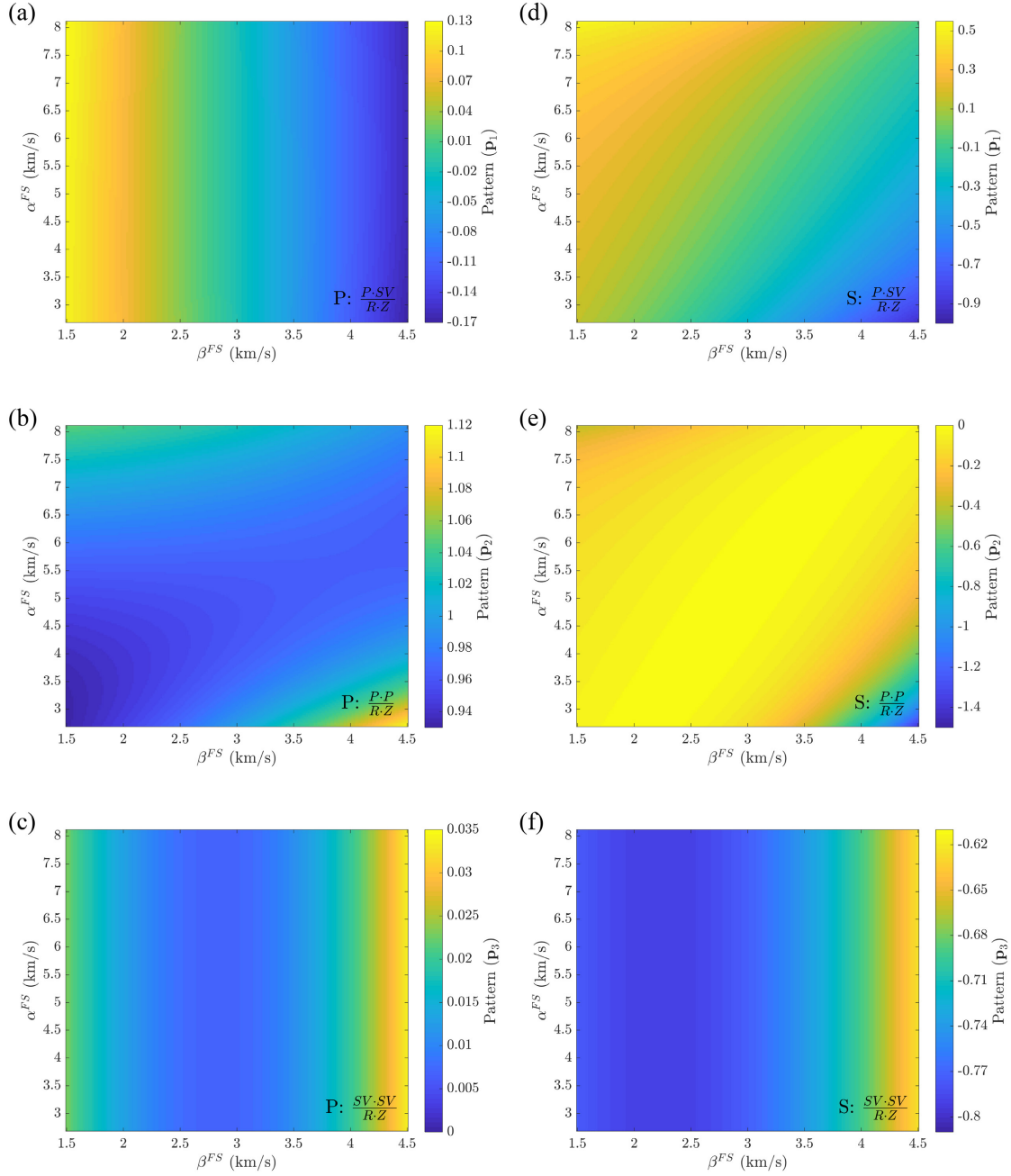[1] Department of Earth, Environmental and Planetary Sciences, Brown University, Providence, RI 02906, USA.

[2] Bullard Laboratories, Department of Earth Sciences, University of Cambridge, Madingley Rise, Cambridge CB3 0EZ, UK.
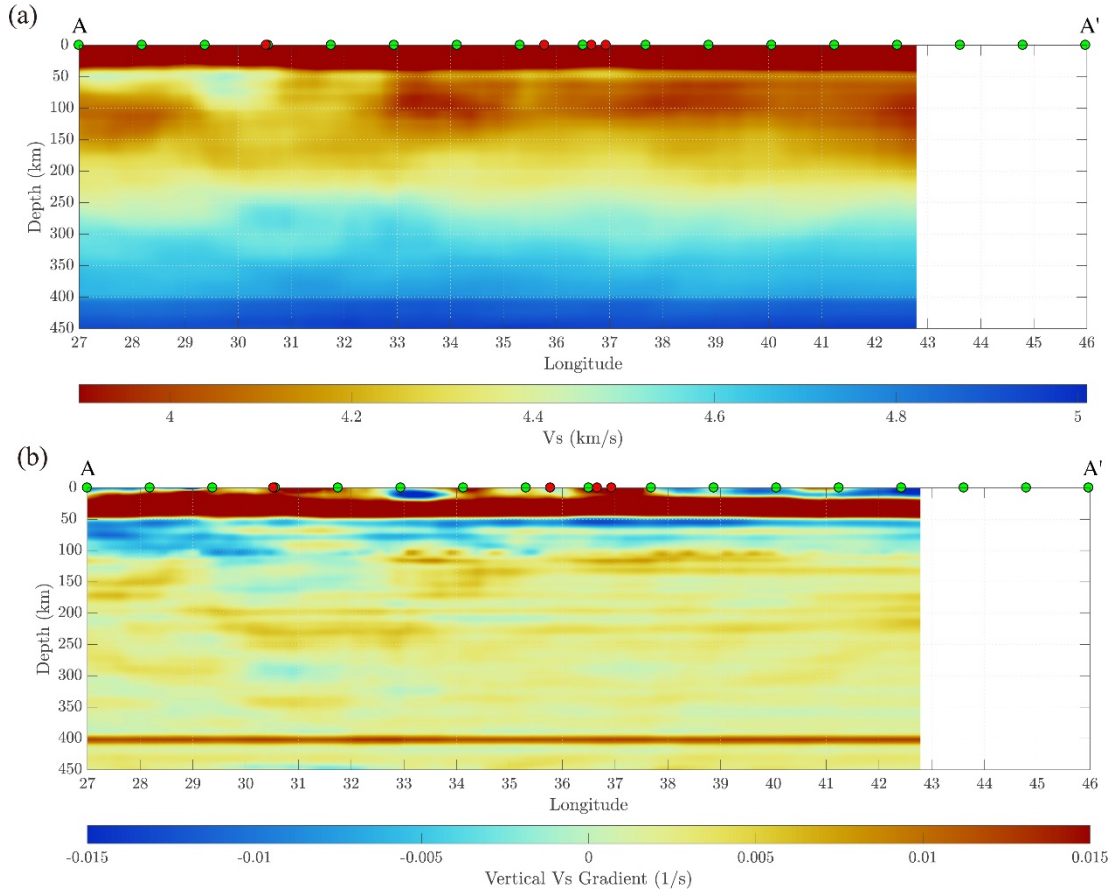
Contents of this file
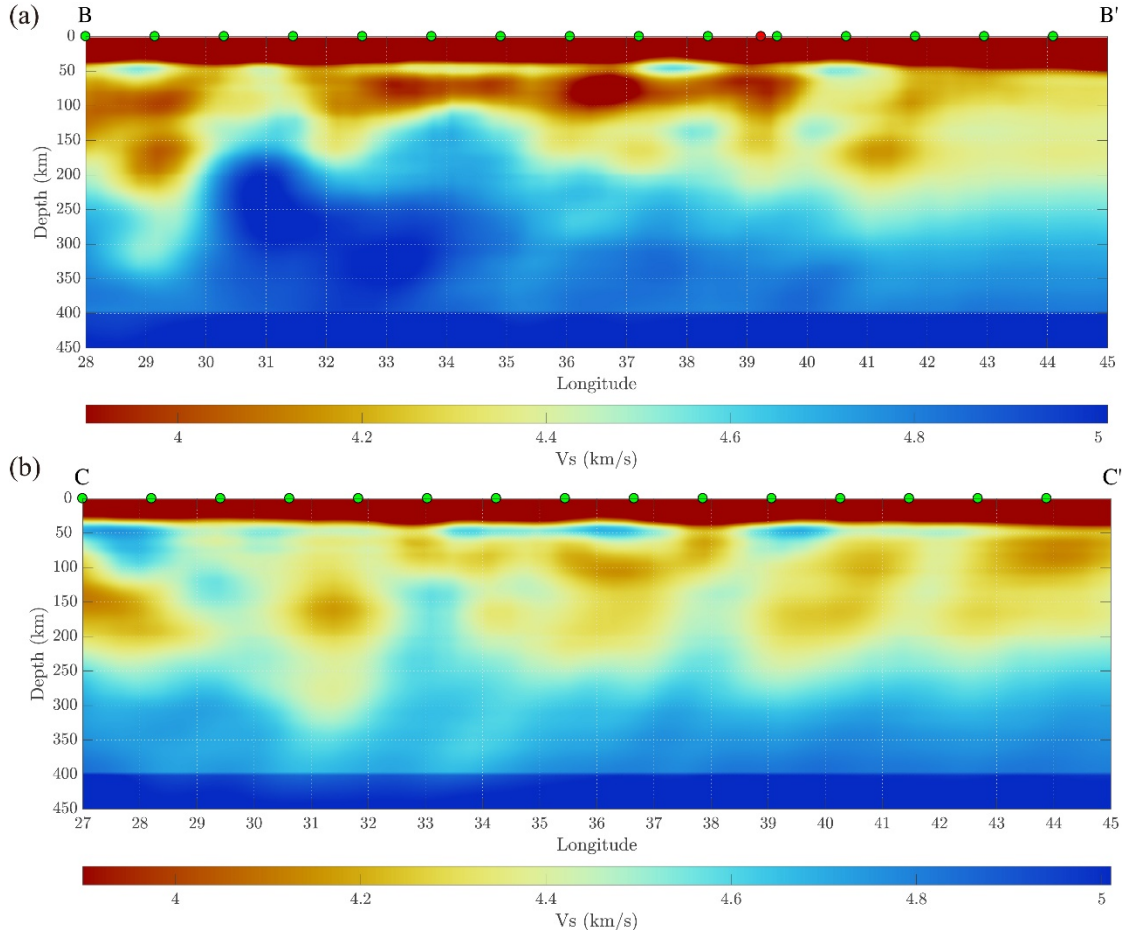
Introduction

This file contains the supplementary figures for the article. Methods used to generate these figures and their interpretation are discussed in the main text.
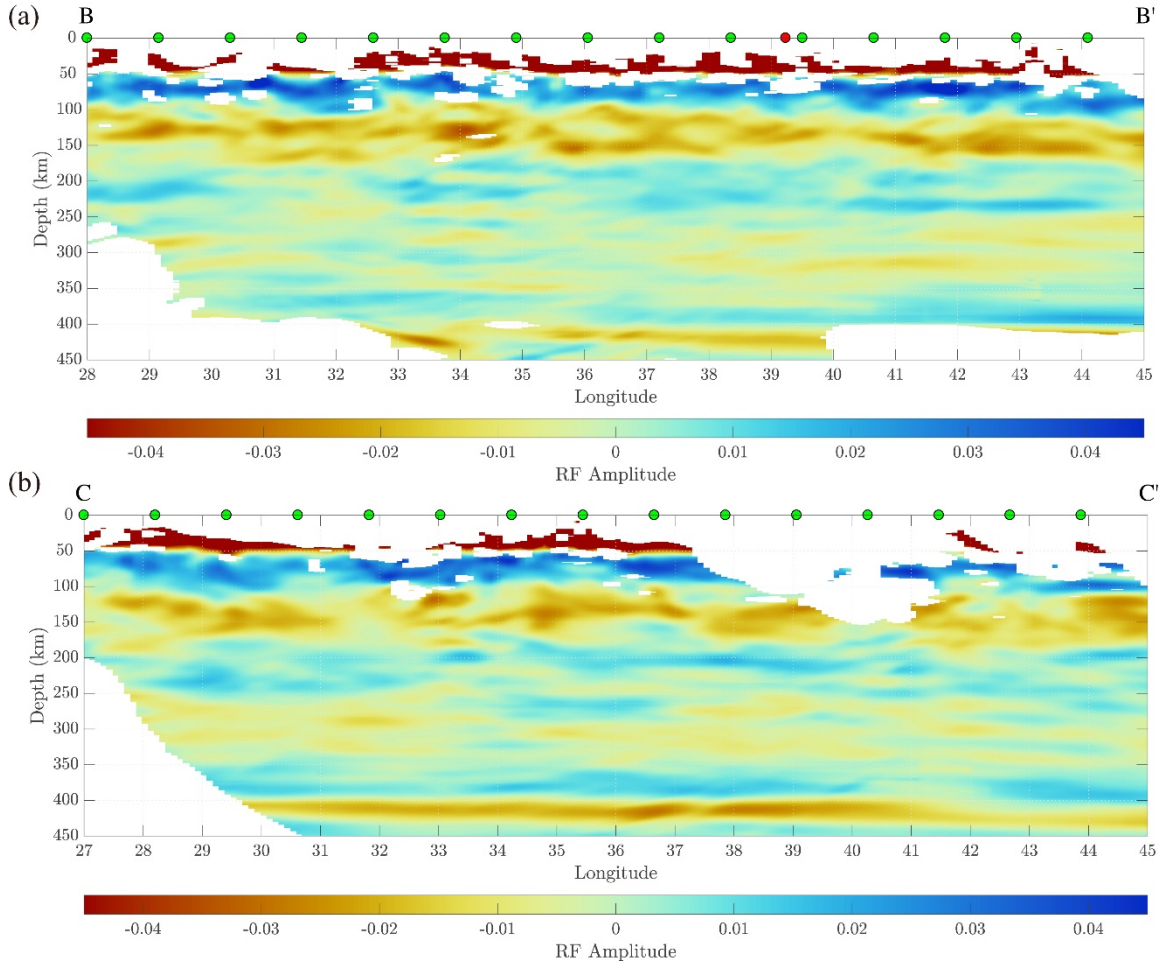
Figure S1. (a)-(c) Particle motion patterns similar to Figures 2a to 2c, but for the real P arrival used in Figure 3. (d)-(f) Particle motion patterns similar to Figures 2e to 2g, but for the real S arrival used in Figure 3. Colors show the value of the pattern for varying α^{FS} and β^{FS}; (a) $\mathbf{C}_1$ pattern; (b) $\mathbf{C}_2$ pattern, (c) $\mathbf{C}_3$ pattern for P arrivals; (d) $\mathbf{C}_1$ pattern; (e) $\mathbf{C}_2$ pattern, (f) $\mathbf{C}_3$ pattern for S arrivals. The label in the bottom right corner indicates the arrival phase and the equation for the pattern.
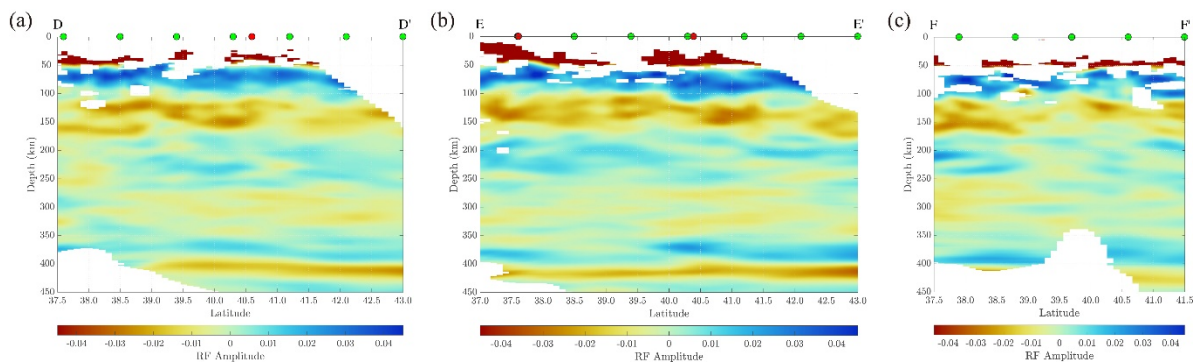
Figure S2. Shear velocity model on profile A-A'. (a) Shear wave velocity from Fichtner et al. (2013). Velocities exceeding the limit of the color bar are shown by the color at the limit (e.g. crustal velocity). (b) Vertical shear wave velocity gradient from Fichtner et al. (2013) smoothed over a 5 km depth window. The velocity model is consistent with the negative Sp phase at depths of 80 – 150 km, in the sense that the velocity model contains a low velocity layer above 150 km depth and positive velocity gradients from 33°E to 40°E at 100 – 130 km depths, but no clear gradients east of 40°E. However, the strong positive velocity gradient at 230 km depth from 29°E to 33°E in the velocity model does not correspond to a feature in the Sp CCP stack.

Figure S3. Shear velocity model on east-west profiles B-B' and C-C' from Blom et al. (2019). Similar to Figure 12a. Velocities exceeding the limit of the color bar are shown by the color at the limit (e.g. crustal velocities). The low velocity layer at 50-110 km depth in (a) broadly agrees with the observed positive velocity gradient in Figure 13a. The absence of a strong low velocity anomaly in (b) agrees with the lack of negative Sp phases in Figure 13b.
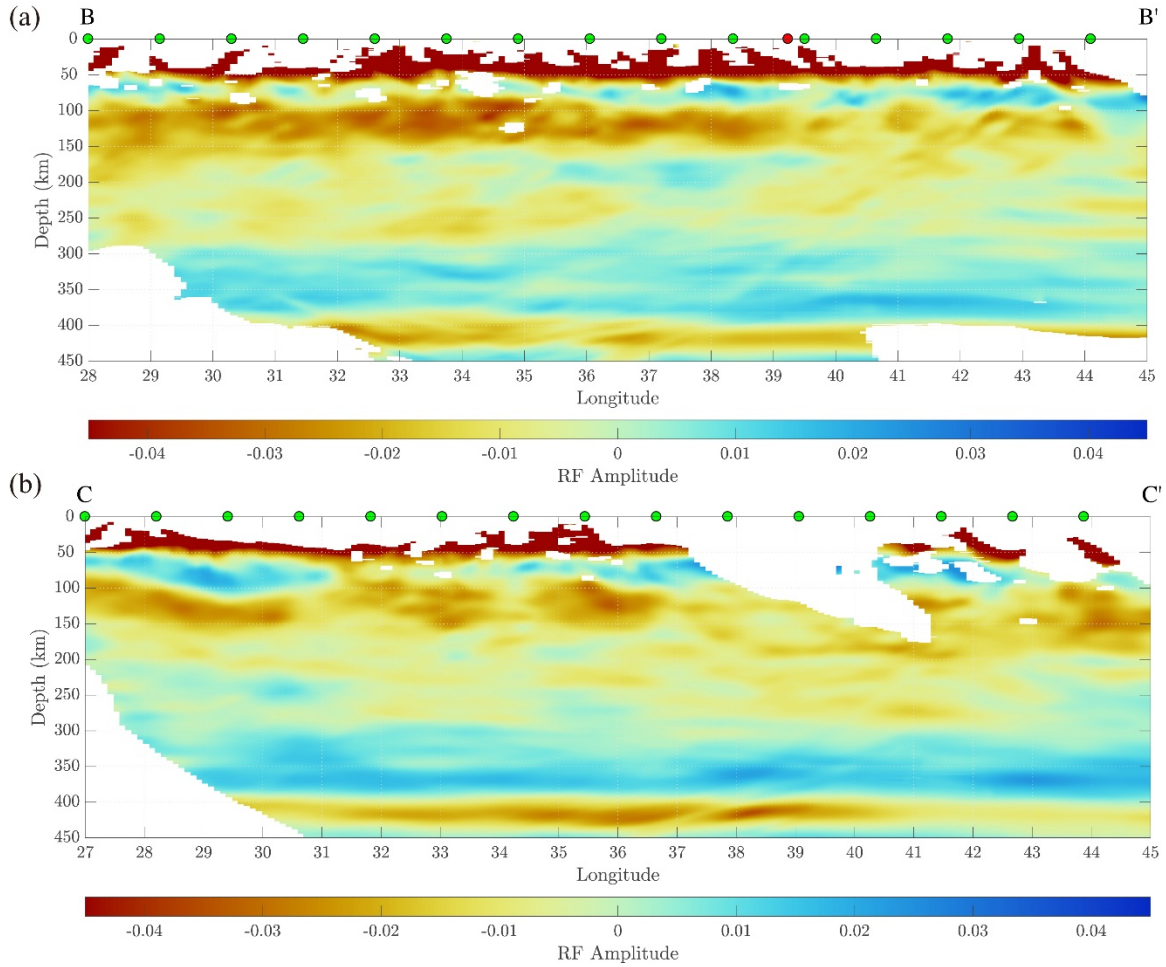
Figure S4. Sp CCP stack amplitudes on east-west profiles B-B' and C-C'. Similar to Figure 13, but using the 2-20 s bandpass filter before deconvolution which is also used in Figure 15a. Symbols and notations identical to Figure 10a. Profile locations shown in Figure 1.
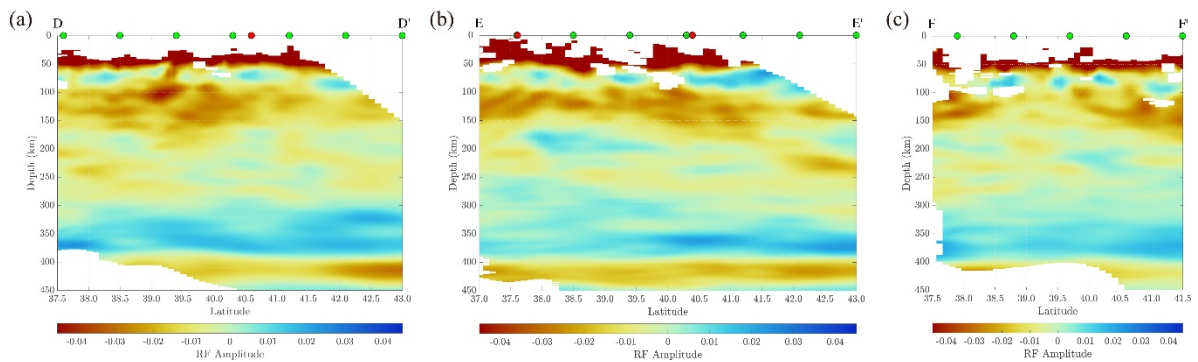

Figure S5. Sp CCP stack amplitudes on north-south oriented profiles D-D', E-E' and F-F'. Similar to Figure 14, but using a 2-20 s bandpass filter before deconvolution. Symbols and notations identical to Figure 10a, but horizontal axes are labeled with latitude. Profile locations shown in Figure 1.

Figure S6. Sp CCP stack amplitudes on east-west profiles B-B' and C-C'. Similar to Figure 13, but using the 10-100 s bandpass filter before deconvolution which is also used in Figure 15b. Symbols and notations identical to Figure 10a. Profile locations shown in Figure 1.

Figure S7. Sp CCP stack amplitudes on north-south oriented profiles D-D', E-E' and F-F'. Similar to Figure 14, but using a 10-100 s bandpass filter before deconvolution. Symbols and notations identical to Figure 10a, but horizontal axes are labeled with latitude. Profile locations shown in Figure 1.